Is Ammonia a Better Solvent Than Water for Contact Ion Pairs?

Germán Sciaini,[†,‡] Ernesto Marceca,[†] and Roberto Fernández-Prini*[,†,§]

INQUIMAE/DQIAQF, Facultad de Ciencias Exactas y Naturales, Universidad de Buenos Aires, Argentina, and UAQ, Comisión Nacional de Energía Atómica, Argentina

Received: May 13, 2008; Revised Manuscript Received: July 13, 2008

The existence of a charge-transfer-to-solvent process when a KI contact ion pair (CIP) dissolved in supercritical water (SCW) is excited by UV light was confirmed by use of electronic structure calculations applied to molecular dynamics trajectories. We observed similar behavior with fluid density as that found for the KI-CIP in supercritical ammonia (SCA); nevertheless, there are some distinct features in the two supercritical solvents. First, the effect of the solvent field due to the molecules lying beyond the first solvation shell is very different in SCW compared with that observed in SCA; in SCW it actually has a destabilizing effect over the ground and excited states. Second, our results for the thermodynamic behavior of the CIP indicate that SCA is better solvent than SCW for this species. The differences found can be attributed to the solvent molecules surrounding the CIP and bridging the two ions; they shield more efficiently the ion pair from long-range solvent effects in SCA. The different behavior is partially attributed to a stronger solvent−solvent interaction in SCW than in SCA.

Introduction

In previous studies we showed that the thermodynamic and spectroscopic behavior of KI contact ion pairs (CIP) dissolved in supercritical ammonia (SCA)[1,2] was mainly determined by the effect of a small number of first-neighbor NH_3 molecules located close to both ions.

A tight solvation structure formed by four ammonia molecules developed around the ion pair as soon as the solvent density was larger than 20% of its critical density; this solvation structure remained almost unchanged when the density of the solution increased. As a consequence, distant solvent molecules had little effect on the local environment of the CIP, and this was evidenced by the very weak density dependence of the photophysical properties of the solution.[3] The solvation behavior observed in SCA solutions of KI for the CIP species differed from those observed for the free ionic species, I^- and K^+, for which the solvation structure was built gradually as the fluid density increased.[2,4]

The study of KI in SCA relied strongly on experimental evidence obtained when KI dissolved in NH_3 at different fluid densities was photoexcited in the UV region and a charge-transfer-to-solvent (CTTS) process occurred. When this happened, an electron was promoted from the solute donor species to a diffuse excited state bound by the interacting solvent field. In recent years,[5] it has been observed that the vertical energy associated with a CTTS transition, as well as the spatial delocalization of the excited electron, provided information about the solvent structure surrounding the ground-state donor species. The extension of the CTTS excited electron density makes this process an interesting probing tool for solvation because it is very susceptible to structural changes occurring in the donor's first solvation shell.

The present work was motivated by the following question: can we expect that the structure of the first solvation shell surrounding a KI-CIP has a similar structure and the same density dependence when the solvent water is used instead of ammonia? Because water is such an important solvent medium, this question is relevant; hence we decided to compare the behavior of KI-CIP observed in SCA with its behavior in supercritical water (SCW).

To answer that question, we studied the CTTS process for KI-CIP in SCW using molecular dynamics (MD) simulations and electronic structure calculations. We determined the fluid density dependence of E_{max}, the maximum energy of electron excitation, and of VDE, the vertical electron detachment energy. The MD runs also gave information about the average solvent structure that surrounds the CIP and allowed us to identify the position of the first-neighbor H_2O molecules located in the intersecting region, that is, H_2O molecules surrounding the CIP and bridging externally the cation with the anion. We hoped the comparison of CTTS features in SCA with those in SCW would help to establish the relative influence of solute−solvent and solvent−solvent interactions in both media. With this purpose in mind, we also determined the effect of long-range solvent interaction upon the CTTS process of CIPs, which was an important feature in the case of KI-CIP in SCA.

Ammonia vis-à-vis Water as Solvents

In order to make clearer the comparison between the two solvents, we start by reporting some properties of the pure solvents. It is known from the information available in the literature that, although NH_3 and H_2O are isoelectronic molecules and capable of forming intermolecular hydrogen bonds, the two liquids have different molecular structures.[6]

Some properties of the two solvent molecules are worth considering. The effective intermolecular potentials employed before for ammonia[7] and for water in the present work[8] show that the charge on each H-atom is very similar for both solvent molecules; this implies that the N atom has 1.5 times more charge than the oxygen atom. Nevertheless, the dipole moments

* Corresponding author. E-mail: rfprini@cnea.gov.ar.
† Universidad de Buenos Aires.
‡ Present address: Institute for Optical Sciences and Departments of Physics and Chemistry, University of Toronto, 80 St. George Street, Toronto, Ontario M5S 3H6, Canada.
§ Comisión Nacional de Energía Atómica.

10.1021/jp8042472 CCC: $40.75
Published on Web 08/27/2008

in the gas phase[9] are $\mu = 4.90 \times 10^{-30}$ C·m (ammonia) and 6.17×10^{-30} C·m (water), and the quadrupole moments are -7.07×10^{-40} C·m^2 (ammonia)[7] and -18.68×10^{-40} C·m^2 (water).[10] These values would suggest that the smaller H_2O molecule in the first solvation shell should be more effective in shielding electrostatically the KI-CIP from the long-range solvent field. On the other hand, the stronger solvent−solvent interaction in water will oppose that tendency. It is important to evaluate which of these two plausible effects predominates upon solvation of the CIPs in SCW by use of the results obtained in SCA for comparison.

Another difference between the two solvents lies in the distinct structures of the fluids, which are due to intermolecular hydrogen bonding. The hydrogen-bond energy, judged by the enthalpy for dimer formation in the vapor phase ($\Delta_{dim}H$), is much stronger in water (−20.84 kJ/mol)[11] than in NH_3, where it is between −13.5 and −12 kJ/mol.[6,12] Liquid ammonia (230 K) has an average of 2.0 H-bonds per molecule,[6] while liquid water (298 K) has ≈3.8.[13,14] Obviously, at supercritical temperatures the average number of intermolecular H-bonds per molecule in both solvents will be appreciably smaller than in the liquid near the triple point, but in H_2O they still persist, albeit in a smaller number. We estimate that water maintains about 1.8 H-bonds per molecule at 673 K.[13−15] NH_3, having a single lone pair of electrons, tends to form hydrogen-bonded domains of restricted size,[6] while H_2O forms a three-dimensional net of H-bonded H_2O molecules. The difference is due to the fact that H_2O molecules have two acceptor and two donor H-bond sites, while NH_3 has only one acceptor H-bond site; this promotes clusters of hydrogen-bonded NH_3 molecules, but no extended dynamic network of bonded molecules exists.

This evidence agrees with the thermodynamic behavior observed for both pure solvents. We studied for both solvents the same corresponding state having the reduced density $\rho_{red} = (\rho/\rho_{1c}) = 1.41$ and reduced temperature $T_{red} = (T/T_{1c}) = 1.04$ ($\rho_{1c} = 17.9$ mol·dm^{-3} and $T_{1c} = 647$ K are the critical density and temperature of the solvent);[16] the fugacity coefficients of both fluids are very similar indeed. However, the situation changes if the enthalpic and entropic terms for the process that takes the solvents from ideal gas to the actual supercritical fluid are compared: the enthalpy is −22.7 kJ/mol for H_2O and −13.1 kJ/mol for NH_3, and the excess entropy term $T\Delta S^{ex}$ is −68.1 kJ/mol for H_2O and −40.6 kJ/mol for NH_3. These values are quite different for the two solvents and they indicate that water, having much larger intermolecular energy than ammonia, is a more extensively structured fluid.

In the case of SCA, it was established that the spectroscopic and thermodynamic behavior encountered for KI at low fluid density was due to the solvation of KI-CIP by four NH_3 molecules surrounding the CIP in the interionic region; this structure was formed already at very low reduced density, $\rho_{red} \geq 0.2$. The change in the electron's excitation route, the negligible effect of long-range interactions on the UV-CTTS band when the supercritical solvent's density changed,[3] and also their remarkable effect upon the solubility of solid KI in SCA[2,17] suggested that these features are due primarily to the four NH_3 molecules that bridge the cation to the anion.

It is important to make a preliminary analysis of the available information on the thermodynamics of electrolytes in SCW. Since no experimental data are available for KI in SCW, we used for comparison the data available for NaCl-CIP in SCW, which is a typical electrolyte. Pitzer and Pabalan,[18] who analyzed the solubility of NaCl (c_2 expressed in moles per cubic decimeter) in vapor-like supercritical water as function of ρ_1, reported values of the enhancement factors (I)[19] for NaCl at 673 and 723 K. We have recalculated them from the original experimental solubility data for SCW at vaporlike densities as detailed below, confirming the very small values of I obtained by linear extrapolation to $\rho_1 \rightarrow 0$, I^{∞}, compared with those found for KI dissolved in SCA[17] under similar conditions. This evidence would indicate that SCA is a better solvent than water for CIPs; that is, it increases more strongly the solubility of the solid salt with the density of the medium.

Since the overall solvation of KI-CIP also is affected by solvent−solvent interactions, which are stronger in water, CIP might be more effectively solvated in ammonia. We will show by means of MD simulations and electronic structure calculations that this is the case; moreover, the energetics associated with the CTTS transition is consistent with the thermodynamic argument. The larger capacity of water to form solvent H-bonded networks may oppose the formation of a specific CIP−solvent aggregate like that observed for the KI−NH_3 system.

Computational Methodology

The values of different electronic properties of KI-CIP dissolved in SCW were obtained by averaging the electronic structure calculations over more than 200 snapshots along classical molecular dynamics trajectories for different solvent densities. This procedure, which combines an efficient classical sampling with quantum electronic calculations, was originally proposed by Bradforth and Jungwirth[20] to describe the CTTS of iodide in bulk water. Very recently, we successfully applied it to model the I^- ion and KI-CIP dissolved in SCA;[3] the value of E_{max} and its fluid density dependence were found to agree satisfactorily with experimental CTTS bands of those two species.[1,4]

Classical Molecular Dynamics Simulations. *NVT* molecular dynamics runs with periodic boundary conditions were performed for one K^+ ion and one I^- ion in a box having 510 water molecules. The solvent density was varied by changing the box's size. Simulations with each single ion were done at an intermediate density to estimate the extension of the first solvation shell, which was considered to be the first minimum of the ion−O radial distribution function; the values 0.385 and 0.490 nm were obtained for K^+ and I^-, respectively. Simulations were performed with AMBER8.[21] Trajectories of 500 ps were computed after 500 ps of thermalization, with a time step of 1 fs and the temperature kept at 673 K, above the critical point.

The rigid SPC/E model[8] was used to describe the solvent. Ion−ion and ion−water interactions were described by Coulombic and Lennard-Jones (LJ) potentials. To determine the ion−O LJ parameters, quantum mechanics calculations were performed for each ion−H_2O pair (see below). Therefore, the LJ coefficients were chosen to match the quantum pair potential as well as the energy and structure at each minimum by performing classical energy minimizations.

Table 1 shows the equilibrium distances K^+−O and I^-−O and the angle O−H···I^- for each corresponding minimum. In the case of the cation, the oxygen of the H_2O molecule was found to point toward K^+, which was located along the C_2 axis of the H_2O molecule.

It should be mentioned that the SPC/E model yields critical parameters for H_2O that are slightly different from the experimental ones;[22,23] however, this small difference does not affect our study, which requires only the absence of liquid−vapor phase transition at the chosen temperature.

Electronic Structure Calculations. Electronic structure calculations were performed with the *Gaussian98* package.[24]

TABLE 1: Comparison of Values for the Minima between H_2O Sites and Ions and Values of the Lennard-Jones Coefficients[a]

	I^-−H_2O		K^+−H_2O	
	MD	ab initio[b]	MD	ab initio[b]
E, kJ·mol^{-1}	−47.78	−48.03	−82.76	−82.76
d_{min}, nm	0.359	0.369	0.266	0.265
angle, deg	33	28		
A, kJ (mol·Å^{12})$^{-1}$	5.86×10^7		2.76×10^6	
B, kJ (mol·Å^6)$^{-1}$	1.76×10^4		5.44×10^3	

[a] According to the equation $V_{ij}(LJ) = A_{ij}/r^{12} - B_{ij}/r^6$. [b] The 6-31++G set was employed for water in the quantum calculations.

The calculations were made following the procedure proposed by Bradforth and Jungwirth[20] for the excited electronic state, which is based upon the assumption that the lowest electronic state having triplet spin multiplicity for the donor species provides a good description of the excited CTTS state of the system. Single reference methods have proven to be very satisfactory in our study of KI in SCA.[2,4] We checked also their validity in SCW by comparing the values obtained for the E_{max} using Hartree−Fock (HF) and Moller−Plesset second-order perturbation theory (MP2) with those calculated by single-excitation configuration interaction, and they were found to agree very well. We used the same basis set for KI as in ref 3 where, in order to describe properly the CTTS excited states, it was crucial that the iodide ion be represented by an augmented basis set including very diffuse functions.

As already shown for KI-CIPs in SCA[1,2] and for I^- in water,[20] the use of a classical point-charge distribution as solvent model is successful in describing the quantities characterizing the electronic excitations, making calculations for hundreds of snapshots feasible. Therefore we decided to represent the water molecules with the same point-charge distribution that they had in the MD simulations, namely, those of the SPC/E model.[8] The results we will show for vertical transition energies are those calculated at MP2 level. The results related to the excited electron distribution—that is, the mean I−e^- distance (vide infra Figure 2)—were done through the use of HF wave functions.[3]

In order to ensure that all electronic properties correspond to KI−CIPs, only those configurations where the distance K−I was shorter than 0.40 nm were taken into account. As the amount of CIPs decreased when the density increased, the MD run was extended by 2 ns when $\rho_{red} = 3.1$ in order to obtain enough snapshots with CIPs.

Results

From the MD trajectories it was possible to calculate the number of solvent molecules in the first solvation shell of KI-CIP. These first neighbors were divided into three regions according to their position relative to CIP, as was done for the same species in SCA:[1] R_{cat} (cationic region), R_{an} (anionic region), and R_{int} (intersecting region containing those solvent molecules bridging the cation and the anion). The extension of each region was determined for SCW in the same manner as for SCA:[1] based on the distances to the first minimum of the radial distribution function between each ion and H_2O molecules. For KI−H_2O we assumed that the anionic and cationic regions extend respectively to the first minima of the ion−O radial distribution functions.

The numbers of first neighbors (N_{fn}) in R_{cat} and R_{int} surrounding KI-CIP in SCW and in SCA are plotted against ρ_{red} in Figure 1.

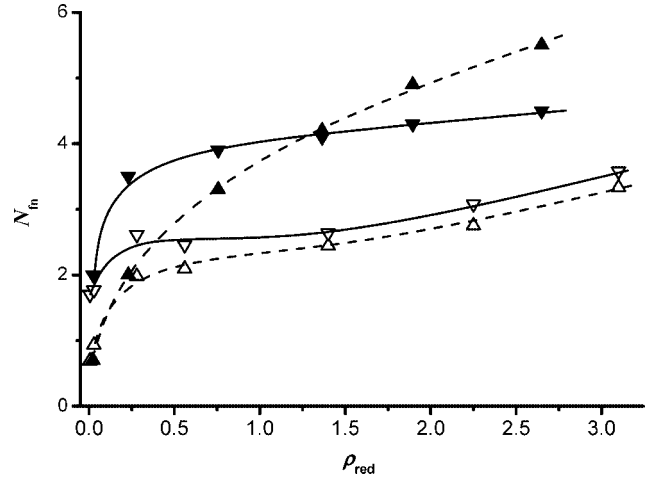

Figure 1. Number of first-neighbor solvent molecules surrounding KI-CIP as a function of ρ_{red}. Solid symbols, SCA; open symbols, SCW. (▲, △) Solvent molecules in R_{cat}; (▼, ▽) solvent molecules in R_{int}. Values of N_{fn} were averaged over 2000 snapshots.

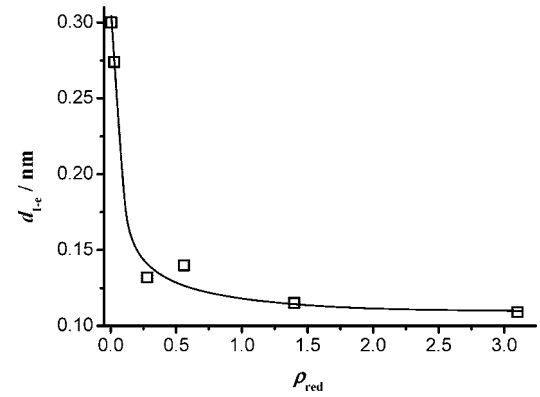

Figure 2. Average mean distance of the excited electron from the iodine nucleus as function of ρ_{red}. Values were obtained by use of the HF wave function as in ref 3.

R_{an}, which is not shown in the figure, exhibits similar behavior in both supercritical solvents. There are two notable differences between the behaviors observed in SCA and in SCW for the first-neighbor solvent molecules, as shown in Figure 1. First, the values of N_{fn} are very different in the two solvents, being much bigger in SCA. In SCW, N_{fn} in R_{int} was around 2.5 until the reduced density exceeded 1.5, and then it increased slowly to 3.6 at the triple-point density. This should be compared with the behavior observed in SCA, where N_{fn} goes from 3.6 to 4.2 as ρ_{red} increased to 2.7.[1,2] Second, N_{fn} in R_{cat} increases smoothly with ρ_{red} in SCA; thus its density dependence is very different from those found for the other three N_{fn} illustrated in Figure 1, which show a steep increase of N_{fn} until ρ_{red} is close to 0.25, and thereafter the numbers of first neighbors vary very little with ρ_{red}, as illustrated by the three curves drawn in the figure.

Our calculations for KI-CIP dissolved in SCW showed that, upon electronic excitation, a broad UV absorption band appeared at the same ρ_{red} where the density dependence of N_{fn} in R_{cat} and in R_{int} changed rather abruptly. The absorption band exhibited the features that characterize a CTTS electronic process and it had a maximum at higher energies than that calculated for the CIP in SCA: nonetheless, the calculated E_{max} shifts to the blue with ρ_{red} in SCW in a similar way to that observed in SCA. The difference in energy of the CTTS bands was also observed for KI dissolved in the liquid solvents, where the excitable species is the free iodide ion.[25] In the supercritical

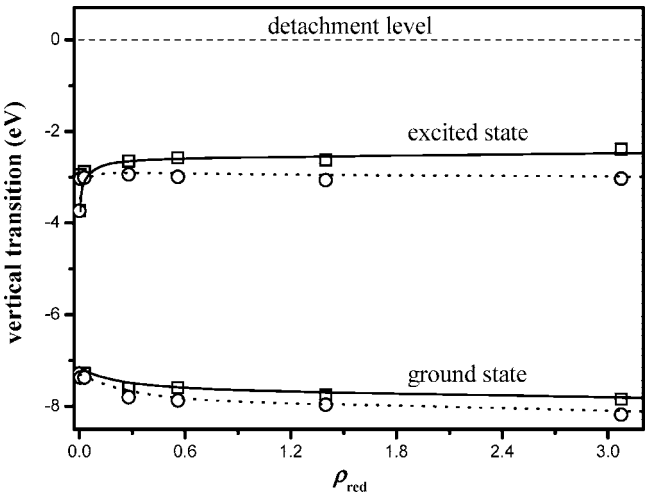

Figure 3. Effect of the long-range solvent field upon electron ground and excited states of KI-CIP as a function of ρ_{red}. (—) All solvent molecules were taken into account; (•••) only first-neighbor H_2O molecules were considered. (---) Value for electron detachment, which was taken as reference for the other states. Calculations were done with MP2.

solvents, where CIP is the predominant donor species, the difference between both solvents was smaller: 0.66 eV for liquid solvents and 0.46 eV for CIPs in supercritical solvents at $\rho_{red} = 1.4$.

There are no great differences in the average distribution and dispersion of the excited electron density in the two solvents; the only notable difference observed was in the average distance of the excited electron from the iodine atom. In SCW this distance decreased sharply with fluid density: already at $\rho_{red} = 0.25$ the average position of the excited electron shifted by almost 0.17 nm from its value in the CIP existing at $\rho_{red} \cong 0.006$ (cf. with half the shift in SCA for the same density change), and then it remained almost constant up to high solvent density. This is illustrated in Figure 2 for KI-CIP in SCW.

The results of the electronic structure calculations also afforded interesting evidence of the differences between the behaviors in both supercritical solvents. In SCA, the electron excitation route of KI-CIP switched from intramolecular charge transfer (ICT) in the vapor phase to CTTS excitation when N_{fn} in R_{int} was around 4, and this first-neighbor structure persisted at all densities. On the other hand, this change of route happens in SCW at a similar value of ρ_{red} when N_{fn} in the same region attains a value of about 2, and this value increases up to 30% when the fluid density is liquidlike. This suggests that for SCW the solvent molecules in R_{int} are more affected by changes in the fluid density than those in SCA. In agreement with this suggestion, a very remarkable difference between SCA and SCW was observed in the effect that the solvent molecules beyond the first solvation shell had on the spectroscopic behavior of KI-CIP in SCW compared with that in SCA.

The change in energies observed in SCW when the long-range solvent effect was taken into account is illustrated in Figure 3.

It is evident that the long-range effect destabilizes CIP in SCW, in both the ground and excited states. This behavior should be compared with the almost negligible effect that the long-range solvent field had on CIP in SCA (cf. Figure 6 in ref 4). In particular the energy of the ground state when only first-neighbor solvent molecules are considered, shown in Figure 3, increases when the long-range effect of the solvent is taken into account, and the change is nearly density-independent. An even

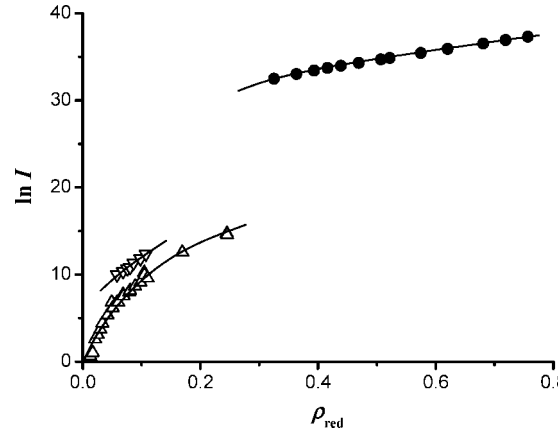

Figure 4. Ln I plotted against ρ_{red} for CIPs in SCA and in SCW. (●) KI in SCA at $T_{red} = 1.04$; (▽) NaCl in SCW at $T_{red} = 1.04$; (△) NaCl in SCW at $T_{red} = 1.12$.

larger destabilization of the excited electron by H_2O molecules beyond the first neighbors was found. We consider that the long-range solvent field effect agrees with the observation that the average distance of the excited electron from the iodine atom is shorter in SCW, thus confining the excited electron closer to the iodine core at lower ρ_{red} in SCW than in SCA.

For free iodide ion, the long-range solvent field in SCA stabilizes the excited electron.[3] If the donor species consisted of the iodide ion plus its first solvation shell, then upon excitation the electron would be detached from the iodine core. Only when solvent molecules beyond the first solvation shell exist was the excited dispersed electron bound to the iodine atom. The long-range solvent field also stabilizes strongly the ground state of I^- in SCA; the same occurs in ambient water for the free I^- donor species.[20]

On the other hand, for CIPs in SCW the long-range solvent effect acts in the opposite direction: it destabilizes the ground and excited states. This observation agrees with the fact that in SCW the values of E_{max} and VDE*, the vertical detachment energy of the excited electron, are sensitive to the field due to solvent molecules lying beyond the first solvation shell. This is a clear indication that the first solvation shell, and especially the molecules lying in R_{int}, screen CIP from the effect of other solvent molecules much more efficiently in SCA than in SCW.

Discussion

First we shall look into the thermodynamic behavior of CIPs in the two supercritical solvents. Since there are no experimental thermodynamic data for KI in SCW, NaCl solutions in that solvent medium were used to establish the typical thermodynamic behavior of CIPs of a simple electrolyte in SCW. We consider this a valid strategy to grasp the general picture of the consequences of the interactions between CIPs and H_2O molecules in SCW. The values reported for ln c_2 of NaCl solutions in low-density SCW at $T_{red} = 1.04$ and 1.12 by Galabardes et al.,[26] including also data of Amellini and Tester[27] for the higher temperature, were fitted as function of ρ_{red}. The lower of these temperatures corresponds to the same reduced temperature for which the solubility of KI in SCA had been determined.[17] From these plots, the values of ln I were linearly extrapolated to $\rho_{red} \rightarrow 0$ to determine I^∞. While at $T_{red} = 1.04$, $I^\infty(\text{NaCl}) = 625$ in SCW, it was $I^\infty(\text{KI}) = 3 \times 10^{11}$ in SCA. At $T_{red} = 1.12$ (corresponding to $T = 723$ K), the data plotted in Figure 4 show a very smooth rise of ln I for NaCl, with ρ_{red} giving $I^\infty(\text{NaCl}) = 2.5$.

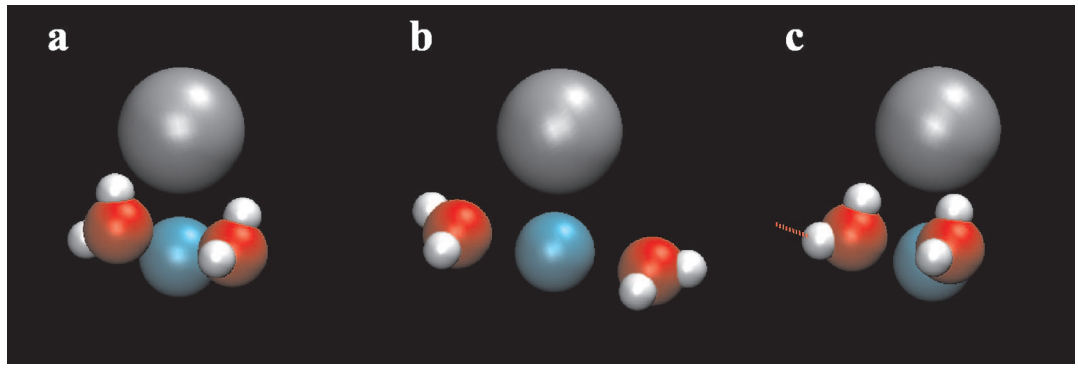

Figure 5. Three representative snapshots of the H_2O molecules in R_{int}. (a, b) $\rho_{red} = 0.3$; (c) $\rho_{red} = 1.4$. Iodide, gray; potassium ion, blue; oxygen atom, red; hydrogen atom, white. Dashed red line indicates hydrogen bonding between first and second shell of H_2O molecules.

The values of ln c_2 in supercritical steam were described by Pitzer and Pabalan[18] using a model of successive ionic association steps; that study also reported relatively modest values of I^{∞} for NaCl-CIP. The values of ln I for KI in SCA are significantly greater than those exhibited by NaCl in SCW; Figure 4 shows that the solubility of KI is strongly enhanced in SCA compared with that in SCW, indicating that the solvent effect is larger in the case of SCA. For NaCl in SCW at the higher temperature, the solubility data approached smoothly the concentration present in pure NaCl vapor. The behavior shown by NaCl in SCW is intermediate between that observed for KI in SCA and those observed for nonionic solutes in nonpolar solvents.[28]

It should be mentioned that our experimental solubility data for KI in SCA could not be determined at sufficiently low ammonia density[4] to overlap the low fluid density range studied for NaCl in SCW. Nevertheless, the use of solubility data at low ρ_{red} in SCW is essential to guarantee that the predominant species in the solution studied experimentally is CIP;[29] in our simulation runs we observed an increasing presence of non-CIP species for KI in SCW when ρ_{red} was above ~0.6.

From the MD trajectories it is possible to give a representative picture of the solvation configurations of KI-CIP at two densities. It is convenient to give here the criteria we used to determine when two H_2O molecules were hydrogen-bonded. We considered two molecules hydrogen-bonded when their O atoms were closer than 0.35 nm and they had an O−H···O angle smaller than 30°.[13]

Figure 5 displays three representative snapshots showing only the position of H_2O molecules in R_{int}. The H_2O molecules in R_{int} often were positioned with an O−H covalent bond parallel to the interionic distance and the second H atom pointing outward (cf. Figure 5a); sometimes H_2O molecules had their oxygen atoms pointing toward K^+ and the two H atoms pointing away from the CIP (cf. Figure 5b). This picture was substantially unaffected by changes in ρ_{red}.

Water molecules inside R_{int} were exceptionally H-bonded to each other. On the other hand, it was often observed that the H_2O molecules inside R_{int} were H-bonded to molecules in the next solvation shell surrounding R_{int} (cf. Figure 5c). The probability of finding H-bonding between molecules in the first two solvation shells was appreciable: 0.25 at $\rho_{red} = 0.3$, growing to 0.5 at $\rho_{red} = 1.4$, and becoming 0.7 at the triple-point density. The number of H-bonds between molecules in R_{int} and those in the second solvation shell per H_2O molecule was more than double that found between molecules in the bulk, and this factor was nearly density-independent. This observation agrees with the idea that the strong H_2O-H_2O interactions effectively compete with the interactions between CIP and water molecules in the first hydration shell.

When the size of the molecules of the two solvents and the magnitude of their dipole and quadrupole moments was taken into account, the smaller number of N_{fn} found in R_{int} in the case of H_2O was rather unexpected. It seems the reason is the magnitude and distribution of charges in the solvent molecules; that is, the molecular features which also lead to hydrogen bonding, as already suggested on the basis of analysis of the relative solvation of small nonpolar molecules in different supercritical fluids.[28] This also would explain the much smaller value of N_{fn} observed in SCW in R_{int} and R_{cat}: those H_2O molecules are strongly influenced by the more distant solvent molecules due to their larger intermolecular interactions. Thus the system studied in the present work emphasizes the role of H_2O-H_2O interactions in fixing the number and strength of interactions of molecules inside R_{int} with CIP.

All this evidence would point to the fact that, in SCA, CIP plus the solvent molecules in R_{int} form a quasi-stable structure, akin to a solvate and that this does not occur in SCW. Thus, in SCA the solvent molecules in R_{int} isolate KI-CIP from long-range interactions more effectively.

Conclusions

The study of the CTTS transition in KI-CIP dissolved in SCW showed a sudden change in the excitation route when ρ_{red} was above 0.25, in agreement with the behavior found for the same species in SCA. However, H_2O molecules in the first solvation shell of KI-CIP that bridge externally the cation with the anion did not shield CIP from the long-range solvation field as efficiently as in SCA. If the detachment threshold is taken as a reference, water molecules beyond the first solvation shell actually increased the energy of the ground and excited electronic states. This difference from SCA is attributed to the much stronger solvent−solvent interaction in SCW. One consequence of this difference is the much larger increase in the solubility of KI-CIP in SCA compared with that in SCW.

Acknowledgment. We are grateful for the economic support given by UBACyT (X218/X330).

References and Notes

(1) Sciaini, G.; Marceca, E.; Fernández-Prini, R. *J. Phys. Chem. B* **2006**, *110*, 8921–8923.
(2) Sciaini, G.; Marceca, E.; Fernández-Prini, R. *Phys. Chem. Chem. Phys.* **2006**, *8*, 4839–4848.
(3) Sciaini, G.; Fernández-Prini, R.; Estrin, D. A.; Marceca, E. *J. Chem. Phys.* **2007**, *126*, 1745041–8.

(4) Sciaini, G.; Marceca, E.; Fernández-Prini, R. *J. Phys. Chem. B* **2005**, *109*, 18949–18955.

(5) Chen, H. Y.; Sheu, W. S. *J. Am. Chem. Soc.* **2000**, *122*, 7534–7542.

(6) Thompson, H.; Wasse, J. C.; Skipper, N. T.; Rayama, S.; Brown, D. T.; Soper, A. K. *J. Am. Chem. Soc.* **2003**, *125*, 2572–2581.

(7) Impey, R. W.; Klein, M. L. *Chem. Phys. Lett.* **1984**, *104*, 579–582.

(8) Berendsen, H. J. C.; Grigera, J. R.; Straatsma, T. P. *J. Phys. Chem.* **1987**, *91*, 6269.

(9) Weast, R. C. *CRC Handbook of Chemistry and Physics*; CRC Press: Boca Raton, FL, 1989.

(10) Eisenberg, D.; Kauzmann, W. *The Structure and Properties of Water*; Oxford University Press: Oxford, U.K., 1969.

(11) Schütz, M.; Brdarski, S.; Widmark, P.-O.; Lindh, R.; Karlström, G. *J. Chem. Phys.* **1997**, *107*, 4597–4605.

(12) Stårling, J.; Schütz, M.; Lindh, R.; Kalström, G.; Widmark, P.-O. *Mol. Phys.* **2002**, *100*, 3889–3399.

(13) Swiatla-Wojcik, D. *Chem. Phys.* **2007**, *342*, 260–266.

(14) Soper, A. K.; Bruni, F.; Ricci, M. A. *J. Chem. Phys.* **1997**, *106*, 247–254.

(15) Franck, E. U. *Structure of Water in Aqueous Solutions*; Proceedings of the International Symposium held in Marburg, Germany, July 1973; Luck, W. A. P., Ed.; Verlag Chemie: Berlin, Germany, 1973.

(16) Lemmon, W. W.; Huber, M. L.; McLinden, M. O. *NIST Reference Fluid Thermodynamic and Transport Properties (REFPROP), version 8.0*; U.S. Department of Commerce, Gaithersburg, MD, 2007.

(17) Sciaini, G.; Marceca, E.; Fernández-Prini, R. *J. Supercrit. Fluids* **2005**, *35*, 106–110.

(18) Pitzer, K. S.; Pabalan, R. T. *Geochim. Cosmochim. Acta* **1988**, *50*, 1445–1454.

(19) *I* is the ratio of the actual solublity in the supercritical fluid to that of the pure solid given by its vapor pressure.

(20) Bradforth, S. E.; Jungwirth, P. *J. Phys. Chem. A* **2002**, *106*, 1286–1298.

(21) Case, D. A.; Darden, T. A.; Cheatham, T. E., III; Simmerling, C. L.; Wang, J.; Duke, R. E.; Luo, R.; Merz, K. M.; Wang, B.; Pearlman, D. A.; Crowley, M.; Brozell, S.; Tsui, V.; Gohlke, H.; Mongan, J.; Hornak, V.; Cui, G.; Beroza, P.; Schafmeister, C.; Caldwell, J. W.; Ross, W. S.; Kollman, P. A. *AMBER 8*; University of California, San Francisco, 2004.

(22) Boulougouris, G. C.; Economou, I. G.; Theodorou, D. N. *J. Phys. Chem. B* **1998**, *102*, 1029–1035.

(23) Hayward, T. H.; Svishchev, I. M. *Fluid Phase Equilib.* **2001**, *182*, 65–73.

(24) Frisch, M. J.; Trucks, G. W.; Schlegel, H. B.; Scuseria, G. E.; Robb, M. A.; Cheeseman, J. R.; Zakrzewski, V. G.; Montgomery, J. A., Jr.; Stratmann, R. E.; Burant, J. C.; Dapprich, S.; Millam, J. M.; Daniels, A. D.; Kudin, K. N.; Strain, M. C.; Farkas, O.; Tomasi, J.; Barone, V.; Cossi, M.; Cammi, R.; Mennucci, B.; Pomelli, C.; Adamo, C.; Clifford, S.; Ochterski, J.; Petersson, G. A.; Ayala, P. Y.; Cui, Q.; Morokuma, K.; Malick, D. K.; Rabuck, A. D.; Raghavachari, K.; Foresman, J. B.; Cioslowski, J.; Ortiz, J. V.; Stefanov, B. B.; Liu, G.; Liashenko, A.; Piskorz, P.; Komaromi, I.; Gomperts, R.; Martin, R. L.; Fox, D. J.; Keith, T.; Al-Laham, M. A.; Peng, C. Y.; Nanayakkara, A.; Gonzalez, C.; Challacombe, M.; Gill, P. M. W.; Johnson, B. G.; Chen, W.; Wong, M. W.; Andres, J. L.; Head-Gordon, M.; Replogle, E. S.; Pople, J. A. *Gaussian 98*; Gaussian Inc.: Pittsburgh, PA, 1998.

(25) Blandamer, M. J.; Fox, M. F. *Chem. Rev.* **1970**, *70*, 59–93.

(26) Galabardes, J. F.; Van Hare, J. R.; Rogers, L. B. *J. Chem. Eng. Data* **1981**, *26*, 363–366.

(27) Amellini, F. J.; Tester, J. W. *Fluid Phase Equilib.* **1992**, *84*, 123–142.

(28) Gutkowski, K.; Japas, M. L.; Fernández-Prini, R. *J. Chem. Thermodyn.* **1997**, *29*, 1077–1086.

(29) Chialvo, A. A.; Simonson, J. M. *J. Chem. Phys.* **2003**, *118*, 7921–29.

JP8042472